UVSQ-SAT, a Pathfinder CubeSat Mission for Observing Essential Climate Variables

Mustapha Meftah, Luc Damé, Philippe Keckhut, Slimane Bekki, Alain Sarkissian, Alain Hauchecorne, Emmanuel Bertran, Jean-Paul Carta, David Rogers, Sadok Abbaki, et al.

remote sensing

MDPI

Article

UVSQ-SAT, a Pathfinder CubeSat Mission for Observing Essential Climate Variables

Mustapha Meftah [1,*], Luc Damé [1], Philippe Keckhut [1], Slimane Bekki [1], Alain Sarkissian [1], Alain Hauchecorne [1], Emmanuel Bertran [1], Jean-Paul Carta [2], David Rogers [3], Sadok Abbaki [1], Christophe Dufour [1], Pierre Gilbert [1], Laurent Lapauw [1], André-Jean Vieau [1], Xavier Arrateig [1], Nicolas Muscat [1], Philippe Bove [3], Éric Sandana [3], Ferechteh Teherani [3], Tong Li [2,4], Gilbert Pradel [2,4], Michel Mahé [5], Christophe Mercier [6], Agne Paskeviciute [7], Kevin Segura [7], Alicia Berciano Alba [7], Ahmed Aboulila [8], Loren Chang [9], Amal Chandran [10,11], Pierre-Richard Dahoo [1] and Alain Bui [12]

1 Université de Versailles Saint-Quentin-en-Yvelines, Université Paris-Saclay, Sorbonne Université (SU), CNRS, LATMOS, 11 Boulevard d'Alembert, 78280 Guyancourt, France; luc.dame@latmos.ipsl.fr (L.D.); Philippe.Keckhut@latmos.ipsl.fr (P.K.); Slimane.Bekki@latmos.ipsl.fr (S.B.); alain.sarkissian@latmos.ipsl.fr (A.S.); Alain.Hauchecorne@latmos.ipsl.fr (A.H.); emmanuel.bertran@latmos.ipsl.fr (E.B.); sadok.abbaki@latmos.ipsl.fr (S.A.); christophe.dufour@latmos.ipsl.fr (C.D.); Pierre.Gilbert@latmos.ipsl.fr (P.G.); laurent.lapauw@latmos.ipsl.fr (L.L.); andre-jean.vieau@latmos.ipsl.fr (A.J.-V.); xavier.arrateig@latmos.ipsl.fr (X.A.); Nicolas.MUSCAT@estaca.eu (N.M.); pierre-richard.dahoo@latmos.ipsl.fr (P.-R.D.)

2 Carta-Rouxel, Campus de l'Innovation des Yvelines, 17 rue Albert Thomas, 78130 Les Mureaux, France; jp.carta@lexat.fr (J.P.-C.); tong.li@aphp.fr (T.L.); pradel@ens-cachan.fr (G.P.)

3 Nanovation, 8 route de Chevreuse, 78117 Châteaufort, France; d.j.rogers@nanovation.com (D.R.); pbo@nanovation.com (P.B.); sandana@nanovation.com (É.S.); fht@nanovation.com (F.T.)

4 CIC1429 INSERM AP-HP, Hôpitaux Universitaires Paris Ile de France Ouest, site R. Poincaré, 104 Boulevard Raymond Poincaré, 92380 Garches, France

5 Radio-club de Saint-Quentin-en-Yvelines F6KRK, 1 bis av. des Frênes, 78180 Montigny le Bretonneux, France; f4dey@ref-union.org

6 AMSAT-Francophone, 14 bis rue des Gourlis, 92500 Rueil Malmaison, France; christophe.mercier@amsat-f.org

7 ISIS—Innovative Solutions In Space B.V., Motorenweg 23, 2623 CR Delft, Netherlands; a.paskeviciute@isispace.nl (A.P.); k.segura@isispace.nl (K.S.); a.berciano@isispace.nl (A.B.A.)

8 ACRI-ST, 260 Pin Montard, Sophia Antipolis, 06410 Biot, France; ahmed.aboulila@acri-st.fr

9 Institute of Space Science and Engineering, Center for Astronautical Physics and Engineering, National Central University (NCU), Taoyuan City 32001, Taiwan; loren@ncu.edu.tw

10 Laboratory for Atmospheric and Space Physics (LASP), University of Colorado, 1234 Innovation Dr., Boulder, CO 80303, USA; Amal.Chandran@lasp.colorado.edu

11 Nanyang Technological University (NTU), 50 Nanyang Avenue, Singapore 639798, Singapore

12 Université de Versailles Saint-Quentin-en-Yvelines (UVSQ), 55 avenue de Paris, 78035 Versailles, France; alain.bui@uvsq.fr

* Correspondence: Mustapha.Meftah@latmos.ipsl.fr; Tel.: +33-1-80-28-51-79

Received: 10 November 2019; Accepted: 20 December 2019; Published: 26 December 2019

Abstract: The UltraViolet and infrared Sensors at high Quantum efficiency onboard a small SATellite (UVSQ-SAT) mission aims to demonstrate pioneering technologies for broadband measurement of the Earth's radiation budget (ERB) and solar spectral irradiance (SSI) in the Herzberg continuum (200–242 nm) using high quantum efficiency ultraviolet and infrared sensors. This research and innovation mission has been initiated by the University of Versailles Saint-Quentin-en-Yvelines (UVSQ) with the support of the International Satellite Program in Research and Education (INSPIRE). The motivation of the UVSQ-SAT mission is to experiment miniaturized remote sensing sensors that could be used in the multi-point observation of Essential Climate Variables (ECV) by a small satellite

constellation. UVSQ-SAT represents the first step in this ambitious satellite constellation project which is currently under development under the responsibility of the Laboratory Atmospheres, Environments, Space Observations (LATMOS), with the UVSQ-SAT CubeSat launch planned for 2020/2021. The UVSQ-SAT scientific payload consists of twelve miniaturized thermopile-based radiation sensors for monitoring incoming solar radiation and outgoing terrestrial radiation, four photodiodes that benefit from the intrinsic advantages of Ga_2O_3 alloy-based sensors made by pulsed laser deposition for measuring solar UV spectral irradiance, and a new three-axis accelerometer/gyroscope/compass for satellite attitude estimation. We present here the scientific objectives of the UVSQ-SAT mission along the concepts and properties of the CubeSat platform and its payload. We also present the results of a numerical simulation study on the spatial reconstruction of the Earth's radiation budget, on a geographical grid of $1^\circ \times 1^\circ$ degree latitude-longitude, that could be achieved with UVSQ-SAT for different observation periods.

Keywords: earth's radiation budget; solar–terrestrial relations; UV solar spectral irradiance; thermopiles; carbon nanotubes; photodiodes; Ga_2O_3; nanosatellite remote sensing

1. Introduction

UltraViolet and infrared Sensors at high Quantum efficiency onboard a small SATellite (UVSQ-SAT) is a Laboratoire Atmosphères, Milieux, Observations Spatiales (LATMOS) nanosatellite mission with scientific and technological goals [1] mainly for observing essential climate variables, namely shortwave and longwave radiative fluxes at the top of the atmosphere and UV solar spectral irradiance. However, the UVSQ-SAT pathfinder mission will not provide a continuity of the essential climate variables' data records since it is a demonstrator. Another objective of the UVSQ-SAT mission is to provide hands-on experience to UVSQ and Paris-Saclay University students in the requirements' definition, reliability and quality assurance, cost and risk management, design, construction, spacecraft integration and testing, mission operations, and control of complete satellite systems that will serve as the basis for a variety of future space missions for Earth observation and astronomy and astrophysics.

The UVSQ-SAT nanosatellite is a cube of about 11 cm with a mass of up to 1.6 kg and a power consumption of up to 2 W. The launch of the CubeSat is currently targeted in the time frame of 2020/2021. The choice of the orbit is directly related to scientific goals while taking into account the optimization for launch opportunities as piggybacking and the rules governing the space debris mitigation. The selected orbit is a Sun-Synchronous (SSO) Low Earth Orbit (LEO) with a maximum altitude of 600 km and a Local Time at Ascending Node (LTAN) of 10:30 hours, which will lead to an atmospheric reentry of the satellite within 25 years. The operational mission lifetime will be at least of one year in orbit, including the commissioning phase, to achieve the expected UVSQ-SAT's scientific objectives.

The first scientific objective of the UVSQ-SAT in orbit demonstration CubeSat is to measure the incoming solar radiation (total solar irradiance) and the outgoing terrestrial radiation (top of atmosphere outgoing longwave radiation and shortwave radiation) using twelve miniaturized Earth radiative sensors (thermopiles based on the advantages of carbon nanotubes and Qioptiq optical solar reflectors). Thus, it might be possible to constrain better the Earth's radiative balance and, more importantly, the Earth's Energy Imbalance (EEI) [2], which is defined as the difference between the incoming solar radiation and the outgoing terrestrial radiation (longwave and shortwave radiation). The EEI's direct determination is very challenging because EEI is two orders of magnitude smaller than the radiation fluxes in and out of the Earth's system.

The second scientific objective is to monitor the solar spectral irradiance in the Herzberg continuum (200–242 nm) using four photodiodes, which benefit from the intrinsic advantages of Ga_2O_3 alloy based sensors grown by pulsed laser deposition [3]. A better understanding of natural factors in

climate variability is the essential motivation of the UV solar spectral irradiance measurements. The UV solar variability over time has significant implications for atmospheric chemistry and its modeling.

The main goal of this paper is to present the UVSQ-SAT mission and the justifications for its existence. Section 2 describes in detail the scientific rationale of the UVSQ-SAT mission. Section 3 provides a description of the UVSQ-SAT nanosatellite and its operational requirements. Section 4 presents a preliminary analysis of the expected results using numerical simulations. The results concern a spatial reconstruction of Earth's radiation budget that might be carried out with UVSQ-SAT data for a given time period of observation. This analysis will also highlight the interest to implement a satellite constellation in order to improve the determination of EEI, which is a crucial quantity for testing climate models and for predicting the future course of global warming. Today, the implementation of an "EEI" constellation based on small satellites is possible. Indeed, the commercial use of small satellites has started thanks to recent advances in miniaturization and integration. Many fields have started benefiting from small satellites: scientific research, technology demonstrations, Earth observations, biological experiments/pharmaceuticals, telecommunications, military applications, etc. Small satellites and the "NewSpace" at Horizon 2020 offer unique opportunities in terms of constellation deployment providing larger simultaneous spatio-temporal coverage of the Earth, which is fundamental for Earth energy imbalance measurements (impacts of aerosols and clouds that are highly variable spatially and temporally).

2. Scientific Rationale of the UVSQ-SAT Mission

2.1. Earth's Energy Imbalance

Currently, Earth's surface temperatures have been rising by about 0.2 K per decade since 1981 [4] (considering deseasonalized monthly surface temperature anomalies from HadCRUTv4.5). Thus, climate change and global warming pose a severe threat to humanity. Climate processes are controlled by energy exchanges within and among the different components of the Earth system. Monitoring the Earth's influx and outflux of both longwave and shortwave radiation from all sources is essential to advance our understanding of climate variability and change and for developing more accurate and reliable climate models and forecasting. Human activities have led to rising levels of heat trapping Greenhouse Gases (GHG) in the atmosphere with less terrestrial radiation being able to escape. This unequivocal anthropogenic radiative forcing of the climate system creates an imbalance in the Earth's energy budget, which causes surface and lower atmospheric warming in order to reestablish a balance in the energy budget [5]. For this reason, EEI represents a measure of the excess of energy that is being stored in the climate system as a response to anthropogenic forcing. As such, it has been identified as a fundamental diagnostic for analyzing climate variability and anticipating future climate changes.

Direct measurements of variations in the energy entering and leaving the Earth system are of primary importance for determining the rate of climate change at regional and global scales [6]. Actually, the most accurate measurement strategy to determine EEI is to monitor the temporal evolution of the ocean heat content since more than 90% of the excess energy that is gained by the Earth in response to the positive EEI accumulates in the ocean in the form of heat [7]. This can be combined with satellite radiation measurements to derive the high frequency variability in EEI. Indeed, the absolute value of EEI can be best estimated from changes in ocean heat content on long timescales, whereas the high spatiotemporal variations in EEI can be provided by satellite observations of net radiation flux variability at the Top Of Atmosphere (TOA). The information on EEI at high spatial and temporal resolution is crucial for advancing our understanding of climate change because the Earth's radiative balance is partly driven by the radiative impacts of aerosols and clouds, which are highly variable spatially and temporally and are still relatively poorly quantified (IPCC, 2014).

Satellites' remote sensing provides a practical and efficient method for mapping Earth's Radiative Balance (ERB) components spatially and temporally at different scales. A large satellite constellation would allow a high frequency and sampling in measurements and consequently a more accurate

determination of the Earth's global energy imbalance along with the diurnal and multi-directional sampling needed to capture spatiotemporal scales relevant to aerosol and clouds (e.g., every three hours and ideally a few km resolution). Advances in small satellite technology now enable the cost effective global solution of monitoring Earth's environment with a minimum constellation of 15 small satellites [1]. Cloud data sharing is a cost effective solution for collecting the constellation data and providing high quality science data in near real time. UVSQ-SAT is one of the first in orbit demonstration CubeSats that is intended to demonstrate the ability to build a low cost satellite with good precision measurements (relative EEI uncertainty at 1σ of $\pm 5\,\mathrm{Wm}^{-2}$ during the mission). Recently, the Radiometer Assessment using Vertically Aligned Nanotubes (RAVAN) 3U CubeSat [8] demonstrated technologies for high accuracy measurement of Earth's radiation budget.

The new UVSQ-SAT concept is designed to explore whether it is possible to achieve the EEI required accuracies using broadband small Earth Radiative Sensors (ERS) onboard multiple satellites (constellation). The main goal of the future satellite constellation is to obtain constant flow of direct measurements from space by using miniaturized instruments (volume, mass, power, telemetry) with narrow and broadband sensors to derive EEI at small spatiotemporal scales with an uncertainty at 1σ of $\pm 1\,\mathrm{Wm}^{-2}$ for a 1–10 km resolution. For longer timescales, EEI direct measurements are also very challenging with a required measurement uncertainty at 1σ of $\pm 0.1\,\mathrm{Wm}^{-2}$ during a decade.

Today, the best estimates of the EEI long term timescales are currently derived from temporal changes in ocean heat content. The global average EEI estimated for the past decades ranges from around +0.4 to +1.0 Wm^{-2} [7,9–12], largely consistent with the radiative forcing caused by anthropogenic greenhouse gases. Hansen et al. [9] inferred a planetary energy imbalance of $+0.58 \pm 0.15\,\mathrm{Wm}^{-2}$ (Earth is absorbing more energy from the Sun than it is radiating to space as heat) during the 6 y period 2005–2010 using ocean heat content. Recently, Johnson et al. [13] estimated EEI at $+0.71 \pm 0.10\,\mathrm{Wm}^{-2}$ for the period May 2005–May 2015 from ocean heat content changes measured by Argo's automated floats. Satellites' measurements from the former generation of Earth Radiation Budget Experiment (ERBE) sensors, along with the current generation of Clouds and the Earth's Radiant Energy System (CERES) sensors are the basis of an ERB multi-decadal record at the top of atmosphere. Currently, CERES sensors provide the most reliable and stable TOA flux measurements of the ERB components.

However, uncertainties in CERES absolute calibration and in the algorithms used to determine ERB from satellite measurements are too large to enable Earth's energy imbalance to be quantified accurately [14]. The CERES data products are more useful for providing the spatial and temporal variability of EEI. Actually, there is a risk of a gap in the ERB data since all current CERES missions are close to the end of their lifetime after 2026 when only tropical missions such as the Franco-Indian Megha-Tropiques or short duration missions such as ESA-JAXA's EarthCARE (Earth Clouds, Aerosols and Radiation Explorer) carry ERB instruments. Indeed, a project intended to complete and replace the CERES instruments by the Radiation Budget Instrument (RBI) mission in 2021, in 2026, and in 2031 was canceled by NASA. Since then, the possibility of a constellation of small satellites in orbit before 2026 is being explored. It represents a major challenge and could meet most of the RBI measurement required for continuity of the climate data records.

To conclude, a measure of the energy imbalance at the top of the atmosphere is crucial, but extremely difficult. It is a key step in the chain linking climate warming to the increase in greenhouse gases. This would be an additional element in the scientific basis for climate change mitigation, notably the magnitude of reduction in GHG emissions required to limit global warming (e.g., 2 °C).

Ideally, accurate long term direct measurements of EEI would confirm the extent of climate warming. Short term measurements of EEI at high spatiotemporal resolution would allow constraining better poorly known radiative forcings associated with aerosols, aerosol–cloud interactions, surface albedo, UV solar irradiance, etc.

The accurate measurements of solar and terrestrial radiative fluxes at TOA over a wide range of surfaces and conditions (e.g., clear-sky, with/without specific clouds or aerosols) would enable a better evaluation of the overall radiative effects of clouds and aerosols and their representations in climate models. Indeed, aerosol and cloud feedbacks arguably remain the dominant source of uncertainties in climate modeling and of its more societally relevant aspects (e.g., changes in precipitation, etc.), as explained in [15,16].

The incoming and outgoing shortwave flux measurements required to calculate EEI also can be used to derive the albedo.

Spatially and temporally resolved albedo measurements allow us to observe the impact of changes in land use, aerosols, and clouds, in terms of the reflection of incident solar radiation back to space, essential for Earth's radiation budget and therefore for the climate.

The spatial and temporal resolution of the radiative measurements determines the scales of the targeted processes. Ideally, the resolution should be high enough to investigate fine scale processes associated with aerosols and clouds, possibly the most important source of divergence between climate models. A 1–10 km resolution would be appropriate for studying local aerosol plumes and clouds. In terms of temporal resolution, being able to follow, even in a crude way, diurnal variations would be a major step forward, in particular for diurnal cycles of clouds or the formation of secondary aerosols (e.g., sulfur, nitrates, which are formed by photochemistry). It is worth pointing out that the albedo issue is at the heart of geo-engineering (or rather, climatic intervention) by solar radiation management, notably using the injection of aerosols or precursors in the atmosphere. High resolution radiative measurements would help to characterize to what extent aerosols affect directly the albedo and indirectly the cloud properties on small scales, today a sort of analogues for geo-engineering. More generally, these measurements would help to carry out process studies on the relationship between initial perturbations and atmospheric response at local scales in terms of shortwave and longwave radiation.

2.2. Solar Spectral Irradiance in the Herzberg Continuum

The role of solar variability in climate variability remains a topic of considerable scientific and societal importance.

Solar radiation is the energy source and is important for the climate. The incoming solar flux or/and its spectral distribution at the top of the atmosphere (due to changes in solar activity or in the Earth's orbital parameters) fluctuate over a wide range of temporal scales, from the 27 day rotational cycle to thousands of years. It also includes 11 y solar cycles and cycles of the order of hundreds of years, called "grand solar minima" and "grand solar maxima".

The solar spectrum [17] and its variability represent key inputs not only for solar physics, but also for climate physics.

Climate models require time varying solar spectra as forcing with the available information often based on solar reconstructions and solar models. There are multiples lines of evidence [18,19] showing that solar variability has been a key forcing in the history of the Earth's climate. Correlations between solar proxies and atmospheric/climate indicators have been established in present day datasets and in sedimentary and ice core archives. However, most of the apparent correlations and associated solar signals tend to be very variable and intermittent. Some are also very difficult to reproduce in climate models.

Establishing a quantitative forcing–response relationship for the Sun–Earth link is problematic without a clear understanding of the key mechanisms engaged in the action of solar variability on the atmosphere and climate, notably at regional scales. There is no general consensus on those mechanisms.

The overall response of the atmosphere and surface climate to solar variability involves a wide range of coupled chemical, dynamical, and radiative processes and the interactions between different atmospheric layers and between the atmosphere and the ocean.

It is worth stressing that the issue of the solar impacts is not just critical for the paleoclimate. It is also highly relevant for the present day climate evolution, which is driven by the GHG rising concentrations. Climate change is a major and growing threat to natural, managed, and human systems. There is already growing evidence for its adverse impacts on the natural environment and human societies (e.g., ecosystems, biological diversity, water resources, and the economy) [20]. There are several sources of uncertainties in climate simulations, in particular in the projections that are used by decision makers to design differentiated mitigation and adaptation strategies [21]. Some of the uncertainties originate from the difficulty to separate the anthropogenic contribution from the natural variability. Quantifying accurately the anthropic contribution and projecting future changes requires understanding and quantifying the natural climate variability including the solar driven variations. It has even been suggested that a new grand solar minimum might occur in the 21st Century [22] and even last until the end of the 22nd Century [23].

The uncertainties are not limited to the mechanisms [18]. They also pertain to the solar variability itself, especially the spectral variations [24]. Indeed, solar forcing is not simply limited to a change in total energy flux. Spectral variations are also important. The relative variations in incoming Solar Spectral Irradiance (SSI) increase very rapidly with decreasing wavelength in the UV range and below. For instance, over an 11 y cycle, the Total Solar Irradiance (TSI) fluctuates by about 0.1% ($\sim$1.4 Wm^{-2}), whereas, in contrast, the radiative flux in the 200 nm region, a key spectral window for stratospheric ozone photochemistry, varies by several %. This has important implications for the way variations in incoming solar energy are redistributed among the different atmospheric layers. The choice of solar UV irradiance variability used to force the models is critical for the solar perturbations of the middle atmosphere [24–26].

The exceptionally weak Solar Cycle 24 and the future Solar Cycle 25 (expected to begin in late 2019) are interesting periods in this context as they might possibly imply the beginning of a general negative solar forcing which would be expected to be vastly outweighed by the global anthropogenic positive forcing [27].

It is also time to clarify better the mechanisms involved in the solar forcing and atmospheric response. The idea is to investigate carefully processes affecting several atmospheric layers. Historically, the impact of solar variability on surface climate has often been seen as resulting only from the direct radiative effects on the Earth's surface and the lower atmosphere. In this framework, the drivers are variations in incoming TSI in wavelength ranges where the middle atmosphere is more or less transparent, i.e., wavelengths longer than 320 nm, corresponding mostly soft UV (UVA), visible, and near-infrared (IR) ranges.

They directly cause changes in the heating rate of the Earth's surface and the lower atmosphere, modifying surface temperatures and climate. At first order, the change in global temperature is essentially due to this direct effect. However, there is also an indirect effect, the so-called "top-down" mechanism (in opposition to the direct effect referred as the "bottom-up" mechanism). In that case, the drivers are variations in the incoming UV flux (below 320 nm) and energetic particles whose energies are almost entirely absorbed by the middle atmosphere. They cause photochemical and dynamic perturbations of the middle atmosphere, which then propagate to the troposphere via stratospheric–tropospheric couplings and result in modifications of surface climate, notably on regional patterns [28–30]. Both mechanisms (top-down, bottom-up) operate at the same time in reality and influence the middle atmosphere and surface climate. An additional complication in studying the top-down mechanism is the fact that UV variations impact the middle atmosphere not only directly via changes in radiative heating, but also indirectly via photochemically driven changes in ozone, the key chemical species and UV absorber in the stratosphere. As a result, the stratospheric temperature response to UV changes is amplified by about a factor of two in a chemistry–climate model (with ozone calculated interactively) compared to the response in the climate model with specified constant ozone [31].

Clearly, the ozone response to solar variability needs to be accounted for in models by treating ozone like temperature, as a variable of the system instead of an input of the model. Only chemistry-climate models can simulate this interaction. Thus, it is necessary to have continuous measurements of the UV solar spectral irradiance with a good accuracy, and particularly in the Herzberg continuum (expected SSI uncertainty at 1σ of $\pm 0.1\%$ per decade) for its influence on stratospheric ozone chemistry. Several missions (Compact Spectral Irradiance Monitor (CSIM) [32], UVSQ-SAT) aim to test the efficacy of a CubeSat making accurate SSI measurements of a much bigger and more expensive satellite.

Indeed, the new UVSQ-SAT concept is designed to see if it is possible to achieve the SSI required accuracies using DEep uV INnovative detector technologies for Space observations (DEVINS) for monitoring UV irradiance variability in the Herzberg continuum. The first step of this strategy is to demonstrate the ability to build the DEVINS sensor, which is a compact/robust/radiation resistant solid-state photodetector that does not require cooling. DEVINS needs to be able to have a functional lifetime higher than classical space based UV sensors [33], which have a limited scientific operating lifetime in weeks rather than months or years due to contaminant trapping by their cooled surfaces [34]. During the UVSQ-SAT lifetime mission, the DEVINS sensor will have to measure the UV irradiance variability in the Herzberg continuum with an uncertainty at 1σ better than $\pm 0.5\%$ and to increase in the future the reliability in the long term data record.

To conclude, there is a need for a better understanding of how the Sun affects the climate, particularly for the UV radiation affecting ozone (the Herzberg continuum) since it links the stratospheric ozone with regional effects. The Herzberg continuum corresponds to a spectral region (200–242 nm) where atmospheric absorption is relatively low and, hence, solar UV radiation penetrates deeply in the atmosphere, down to the lower stratosphere, where it converts molecular oxygen (O2) by photolysis to produce ozone (O3). Absolute solar spectral irradiance and variability in the Herzberg continuum are necessary to better understand the stratospheric ozone response to solar UV irradiance changes [35]. This is important because the Sun has long term and short term variations, and we need to know how these interact with anthropogenic effects. It is also important to understand natural factors in climate variability to give a basis for a future where it might be predicted. The accurate measurements of the solar spectrum at the top of the atmosphere and its variability are fundamental inputs for Earth's climate (climate modeling) and terrestrial atmospheric photochemistry. This is also important for long term variations of solar cycle minima, which are of fundamental importance for solar physics modeling (dynamo, energy transfer, magnetic and 11 y cycles, etc.). Thus, it is necessary to monitor continuously the Herzberg continuum region over years [36]. One of the objectives of the UVSQ-SAT mission is to validate a new technology for future continuous UV observations using small satellites.

2.3. Scientific Requirements

As explained in detail in Section 2.1, measuring the absolute value of the Earth's energy imbalance and its variability over time appears to be a very difficult challenge. The relevant scientific goal is to be able to detect any long term trend with a target accuracy of 1/10 of the expected signal of 0.5–1.0 Wm^{-2} in the global mean during a decade [10–12]. This issue could be solved through better absolute calibration of the sensors since several satellites will be needed to carry out these measurements with satellites' temporal overlap to realize inter-calibrations. Table 1 presents the scientific objectives to be achieved by future space based instrumentations onboard small satellites with onboard calibration systems for EEI observations. These EEI scientific objectives are extremely relevant and have not been achieved so far. At the present stage, the UVSQ-SAT CubeSat is a demonstrator, expecting future developments and improvement that would then really allow making use of CubeSat technology for these scientific purposes. EEI expected performances of the UVSQ-SAT CubeSat are given in Table 1.

Table 1. Scientific requirements for Earth's energy imbalance and solar spectral irradiance in the Herzberg continuum (high scientific relevance and UltraViolet and infrared Sensors at high Quantum efficiency onboard a small SATellite (UVSQ-SAT) expected performances). EEI, Earth's Energy Imbalance; SSI, Solar Spectral Irradiance.

Requirements	**Scientific Relevance**	
Essential Climate Variable (ECV)	Absolute uncertainty	Stability per decade
EEI measurements	$\pm 1\,Wm^{-2}$ at 1σ	$\pm 0.1\,Wm^{-2}$ at 1σ
SSI at 215 nm	$\pm 1.7\,10^{-4}\,Wm^{-2}nm^{-1}$ ($\pm 0.5\%$ at 1σ)	$\pm 3.4\,10^{-5}\,Wm^{-2}nm^{-1}$ ($\pm 0.1\%$ at 1σ)
Requirements	**UVSQ-SAT Performances**	
Essential Climate Variable (ECV)	Absolute uncertainty	Stability per year
EEI measurements	$\pm 15\,Wm^{-2}$ at 1σ	$\pm 5\,Wm^{-2}$ at 1σ
SSI at 215 nm	$\pm 8.5\,10^{-4}\,Wm^{-2}nm^{-1}$ ($\pm 2.5\%$ at 1σ)	$\pm 1.7\,10^{-4}\,Wm^{-2}nm^{-1}$ ($\pm 0.5\%$ at 1σ)

The absolute value of UV SSI and its variability during more than one decade are also challenging (Section 2.2). Accurate observations are fundamental to consolidate the reconstruction models of the solar spectral irradiance. Spectral And Total Irradiance REconstruction for the Satellite Era (SATIRE-S) [37] highlights a weak long term trend (Figure 1) of UV solar spectral irradiance over the past 40 years for solar minima (inter-cycles), which can be real or not.

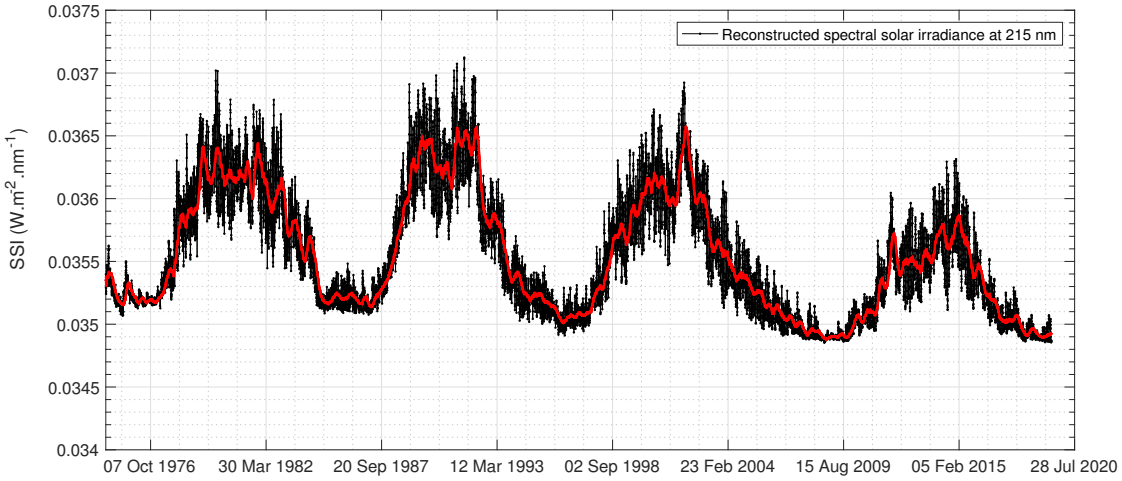

Figure 1. UV solar spectral irradiance at 215 nm over the past 40 years from the SATIRE-S model.

The relevant scientific goal is to be able to detect any long term trend with a target stability per decade of $\pm 3.4\,10^{-5}\,Wm^{-2}nm^{-1}$ (Table 1) at 215 nm ($\sim$1/10 of the expected trend (Figure 1) of the inter-cycles during a decade).

These solar observations with satellites temporal overlap to realize inter-calibrations are important since an analysis of radionuclides [23] concluded that the Sun will enter a state of significantly lower activity within the next 50 to 100 years. These accurate observations are also important for long term reconstructions over centuries where only proxies of solar activity are available as input for the reconstruction models. Indeed, the physical assumptions that go into the models lead to considerable discrepancies [38]. At the present stage, the UVSQ-SAT CubeSat is a demonstrator that must show that these accurate SSI continuous measurements are possible with small satellites using new compact and robust disruptive technologies. UV solar spectral irradiance in the Herzberg continuum expected performances of the UVSQ-SAT CubeSat are given in Table 1.

3. Materials and Methods

UVSQ-SAT is a LATMOS mission based on the deployment of one CubeSat and with the goal to monitor essential climate variables. The UVSQ-SAT mission contains a space segment and a ground segment that uses at least one UHF/VHF antenna located at Observatoire de Versailles Saint-Quentin-en-Yvelines (France). The ground segment includes all the activities from CubeSat monitoring/control to data product generation and distribution.

3.1. The Space Segment: The UVSQ-SAT CubeSat Platform

UVSQ-SAT is a nanosatellite development project underway based on the CubeSat standard [39,40]. UVSQ-SAT is a one Unit (1U) CubeSat designed to provide a 11.10 cm ×11.10 cm ×11.35 cm useful volume (stowed configuration). LATMOS is a prime contractor of the 1U CubeSat with the support of a manufacturer (Innovative Solutions In Space (ISIS)) to build a dedicated satellite platform. Although the CubeSat is small, it contains all the critical subsystems and functions present in larger satellites. A configuration of the UVSQ-SAT nano-satellite is shown in Figure 2, and an overview of the UVSQ-SAT CubeSat properties is given in Table 2. Appendix A provides more details about the satellite platform architecture.

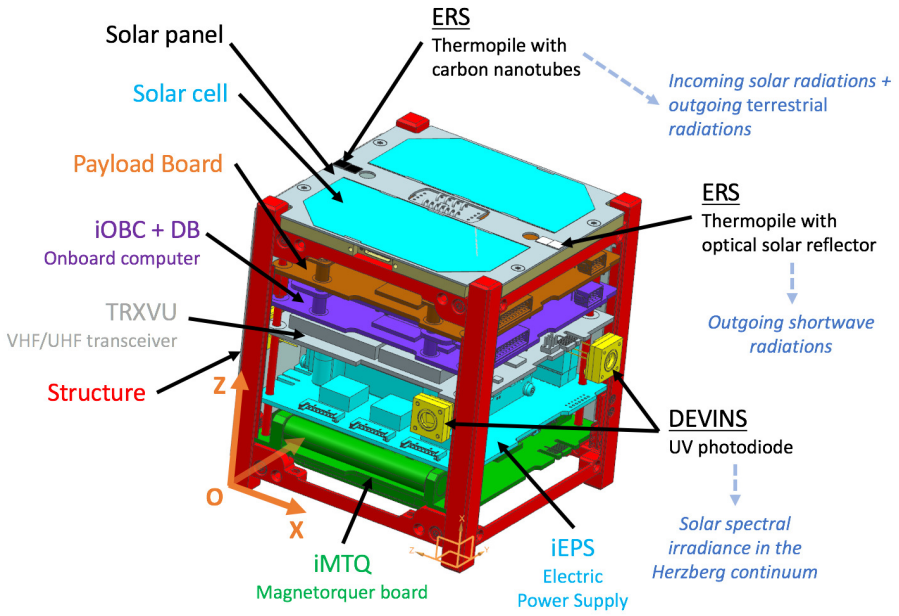

Figure 2. UVSQ-SAT computer aided design representation with an arrangement of all Printed Circuit Boards (PCBs). The UVSQ-SAT payload instruments are shown (Earth Radiative Sensors (ERS) and DEep uV INnovative detector technologies for Space observations (DEVINS)), except the three axis accelerometer/gyroscope/compass, which is located above the payload electronic board.

Table 2. UVSQ-SAT CubeSat properties.

Properties	Value	Comments
Orbit	SSO	Maximum altitude of 600 km, LTAN of 10:30
Design lifetime	1 year for LEO	3 years desired
Launch date	Q4 2020/Q1 2021	Launch vehicle: Soyuz
Size	1U	11.10 cm (X) ×11.10 cm (Y) ×11.35 cm (Z)
Mass	1.6 kg	Maximum with margins

Table 2. *Cont.*

Properties	Value	Comments
Solar cells	12	3G30A solar cells provided by Azurspace
Batteries	22.5 Wh at 8 V	2 Panasonic batteries (NCR18650B) with heaters
Power generated	2.2 W	Orbit average power per 1U area in LEO
Power consumption	1.6 W	Maximum orbit average with margins
ADCS (Appendix A)	3 axis magnetometer	Measurements of the local Earth magnetic field
	3 axis magnetorquer	0.2 Am^2 magnetic dipole
	6 SLCD-61N8 photodiodes	Coarse estimation of the Sun's direction (θ)
CDHS and OBC (Appendix A)	400 MHz, 32-bit ARM9	Processor
	32 MB SDRAM	Synchronous Dynamic Random Access Memory
	2×2 GB SD cards	Non-volatile Data Storage (SD card redundancy)
	1 MB NOR flash memory	Code storage
	I^2C, SPI, UARTs	UART is only used for debugging iOBC
Data downlink	1.2/9.6 kbps	UHF BPSK (437.020 MHz) communication
Data uplink	9.6 kbps	VHF FSK (145.830 MHz) communication
Ground contact station	Less than 1 hour per day	LATMOS station
Redundancy stations	NCU (TW), ACRI-ST (FR)	Other stations: amateur radio partners
Downlink UVSQ-SAT data	1.8 Mbyte per day	Maximum during a day
Uplink UVSQ-SAT data	0.3 Mbyte per day	Maximum during a day
Transponder	Link with amateur radio	Live retransmission of FM signals
Payload	12 ERS	EEI measurements
	4 DEVINS	UV SSI measurements
	1 Teach' Wear (TW) sensor	Accelerometer, gyroscope, and compass
Launch adapter	ISIPOD or Quadpack	CubeSat deployer with a satellite mass up to 2 kg

3.2. The Space Segment: The UVSQ-SAT CubeSat Payload

3.2.1. The ERS Sensors

To measure with accuracy the incoming solar radiation (TSI) and the Earth Outgoing Radiation (EOR = top of atmosphere Outgoing Longwave Radiation (OLR) + Shortwave Radiation (OSR)), we will use new Earth Radiative Sensors (ERS).

ERS are sensors based on miniaturized thermopiles (active area of 5 mm × 5 mm, responsivity of $\sim 0.2\ \mu$ V per Wm^{-2}) designed to measure the heat flux from a 180° field of view angle. The passive (cold) junctions of the thermopile are fully protected from radiation and in thermal contact with the UVSQ-SAT structure, which serves as a heat-sink. Figure 3 shows the measurement principle of these sensors. UVSQ-SAT uses an ERS sensor with carbon nanotubes and an ERS sensor with an optical solar reflector on each side of the CubeSat (Figure 2).

The ERS sensors with carbon nanotubes will absorb all incoming solar radiation and outgoing terrestrial radiation. They have a flat spectrum from UV up to 100 µm, and have a near-perfect cosine response. The carbon nanotubes used (Vantablack from Surrey NanoSystems) are one of the darkest substances known, absorbing up to 99.964% at 700 nm if the light is perpendicular to the material. These carbon nanotubes show excellent Bidirectional Reflectance Distribution Function (BRDF) performances for different incident angles and different scatter angles (total integrated scatter of 0.94% with an angle of incidence of 70°). The ERS sensors with an optical solar reflector will absorb mainly top of atmosphere outgoing longwave radiation. They have a high reflectance from UV up to 3 µm. They were selected since the variation of solar absorptance due to environmental exposure (thermal cycling, UV radiation, protons, etc.) is extremely weak.

The performances of the coatings (carbon nanotubes and optical solar reflectors) were measured using a spectrophotometer (Agilent Cary 5000 UV-NIS-NIR) to obtain the solar absorption (between 200 and 2500 nm), an IR reflectometer (model DB100) to obtain the IR normal emittance (around 10 µm),

and a goniophotometer (REFLET 180S) to obtain the BRDFs (five angles of incidence (0°, 30°, 36°, 60°, 72°) in the 400–800 nm wavelength range in steps of 10 nm).

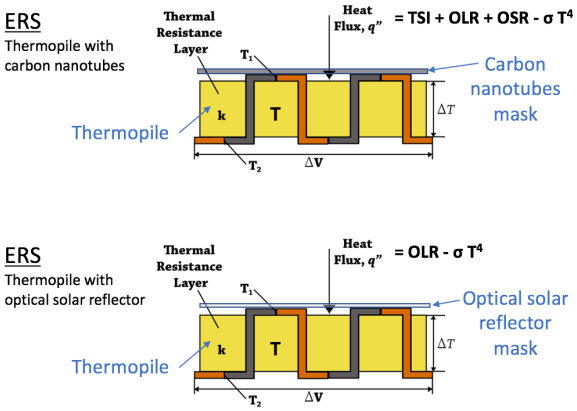

Figure 3. Earth Radiative Sensors (ERS) measurement principle. On each side of UVSQ-SAT, there are these two sensors. TSI, Total Solar Irradiance; OLR, Outgoing Longwave Radiation; OSR, Outgoing Shortwave Radiation.

The large field of view of both sensors on each side of UVSQ-SAT allows measuring all fluxes (TSI, OLR, OSR, black-body flux of the sensor (σT^4), residual fluxes (Moon, planets, etc.)). Considering that we know the value of the solar flux (TSI measurement obtained from space based solar radiometers), the sensors' temperatures (UVSQ-SAT housekeeping data), the residual fluxes (ephemerides of various bodies of the solar system obtained from Institut de mécanique céleste et de calcul des éphémérides (IMCCE)), then we can determine OLR and OSR from a two equation System (S) based on the following thermo-dynamical equations using 12 nodes (N = 12 thermopiles).

$$C_i \frac{\partial T_i}{\partial t} = A_i \cos(\theta_i) \frac{d^2}{d_{Sat-S}^2} \int_\lambda SI(\lambda)\alpha_i(\lambda)d\lambda + A_i F_{i-Earth} \int_\lambda \varepsilon_i(\lambda) EI(\lambda) d\lambda + A_i \frac{d^2}{d_{Sat-S}^2} F_{i-a} \int_\lambda aSI(\lambda)\alpha_i(\lambda)d\lambda + \sum_{j=1}^{N} GL_{i-j}(T_j - T_i) + \sigma \sum_{j=1}^{N} GR_{i-j}(T_j^4 - T_i^4) + Qr_i \quad (1)$$

where i is an ERS thermopile element, C_i is the capacitance of thermopile i (J/K), T_i is the temperature of thermopile i (K), t is the time (s), A_i is the surface area of thermopile i (m^2), θ_i is the angle between the solar direction and the normal of the thermopile, d is the Earth-Sun distance (km), d_{Sat-S} is the spacecraft-Sun distance (km), $SI(\lambda)$ is the spectral solar irradiance in $Wm^{-2}\mu m^{-1}$, λ is the wavelength in μm, $\alpha_i(\lambda)$ is the solar absorption of thermopile i, $F_{i-Earth}$ is the Earth view factor, $\varepsilon_i(\lambda)$ is the normal emittance of thermopile i, $EI(\lambda)$ is the spectral Earth irradiance in $Wm^{-2}\mu m^{-1}$, F_{i-a} is the albedo view factor, a is the Earth's albedo, GL is the conductive couplings of thermopile i (W/K), GR is the radiative couplings of thermopile i (W/K) σ is the Stefan–Boltzmann constant (5.6704 $\times 10^{-8}$ $Wm^{-2}K^{-4}$), and Qr_i is the absorbed residual power (Moon, planets, etc.). This yields solving a set of N differential non-linear equations to obtain OLR $\left(\int_\lambda EI(\lambda)d\lambda\right)$ and OSR $\left(\int_\lambda a\, SI(\lambda)d\lambda\right)$ data without having knowledge of the satellite's attitude.

Then, for ERS data processing, the first step will consist of developing deep learning methods to estimate the attitude of the UVSQ-SAT CubeSat using all housekeeping data (platform and payload inertial measurement units, three axis payload compass, coarse platform photodiodes for solar orientation, power on each solar panel, etc.). Indeed, UVSQ-SAT does not have an active Attitude Determination and Control System (ADCS), which allows precise pointing of the CubeSat. This is one of the reasons why the UVSQ-SAT CubeSat is equipped with broadband ERS sensors (with a large field of view) on each side. For a second time, we will determine top of atmosphere OLR and OSR as a time

function from the rough preliminary equations System (S) given below, originating from Equation (1). The total solar irradiance will be considered as known and obtained from space based radiometers.

$$C_{1a} = \sum_{i=1}^{6} \left(\varepsilon_{K_2,i}\, \sigma(T_{K_2,i}^4 - T_s^4) + \frac{U_{K_2,i}}{S_{K_2,i}} \right) \tag{2}$$

$$C_{1b} = \mathrm{TSI}\, \frac{d^2}{(1\mathrm{u.a.})^2} \frac{1}{\left(1 - \frac{1}{c}\frac{\partial z}{\partial t}\right)^2} \tag{3}$$

$$C_{1c} = \left(\frac{R_E^2}{(z+R_E)^2} + \frac{4}{\pi} \left(\arctan\left(\frac{1}{\sqrt{h^2-1}} \right) - \frac{\sqrt{h^2-1}}{h^2} \right) \right) \tag{4}$$

$$Fv_a = \cos^{1.5}(0.9\,\Theta_s)\; C_{1c} \tag{5}$$

$$\mathrm{OLR}_{K_2} \simeq \frac{C_{1a} - (a_0\, Fv_a + 1)\; < \alpha_{K_2,i} >\; C_{1b} - Qr_i / A_i}{< \varepsilon_{K_2,i} >\, C_{1c}} \tag{6}$$

$$C_{2a} = \sum_{i=1}^{6} \left(\varepsilon_{K_1,i}\, \sigma(T_{K_1,i}^4 - T_s^4) + \frac{U_{K_1,i}}{S_{K_1,i}} \right) \tag{7}$$

$$a_{K_1} \simeq \frac{C_{2a} - \mathrm{OLR}_{K_2}\; < \varepsilon_{K_1,i} >\; C_{1c}}{< \alpha_{K_1,i} >\; C_{1b}\, Fv_a} - \frac{1}{Fv_a} \tag{8}$$

where $\varepsilon_{K_1,i}$ is the carbon nanotubes' emissivity, $\varepsilon_{K_2,i}$ is the optical solar reflector emissivity, $T_{K_1,i}$ is the temperature of the K_1, i thermopile, $T_{K_2,i}$ is the temperature of the K_2, i thermopile, T_s is the deep space temperature, $U_{K_1,i}$ is the voltage of the K_1, i thermopile, $U_{K_2,i}$ is the voltage of the K_2, i thermopile, $S_{K_1,i}$ is the responsivity of the K_1, i thermopile, $S_{K_2,i}$ is the responsivity of the K_2, i thermopile, R_E is the Earth's radius, z is the satellite altitude, a_0 is the initial albedo value (0.3), a_{K_1} is the albedo value obtained after iteration $(a_{K_1} - a_0) < 10^{-5}$, $\alpha_{K_1,i}$ is the carbon nanotube absorptivity, $\alpha_{K_2,i}$ is the optical solar reflector absorptivity, TSI is the total solar irradiance, d is the satellite-Sun distance, 1a.u. is one astronomical unit, c is the speed of light in a vacuum, and Θ_s is the satellite-Earth-Sun angle.

Using this set of equations (S), the UVSQ-SAT scientific target can be obtained without active ADCS (nadir satellite pointing). Thus, we will be able to provide a reconstruction of a global map of top of atmosphere outgoing longwave radiation and another map for outgoing shortwave radiation (binned into a $1^\circ \times 1^\circ$ latitude-longitude geographic grid and averaged over several days of observations).

The UVSQ-SAT EEI expected performances (Table 1) depend on the error budget of the ERS sensors. Absolute uncertainties of each parameter of the system (S) are given in Table 3. The targeted characteristics of ERS thermopiles and temperature sensors are provided in Table 4.

Table 3. Error budget of the ERS sensor.

Uncertainty Sources	Absolute Uncertainty	Determination Method
Emissivity ($\varepsilon_{K_1,i}$, $\varepsilon_{K_2,i}$)	±0.25%	Ground based calibration, BRDF
Absorptivity ($\alpha_{K_1,i}$, $\alpha_{K_2,i}$)	±0.25%	Ground based calibration, BRDF
Temperatures ($T_{K_1,i}$, $T_{K_2,i}$)	±0.01 Kelvin	Ground based calibration, in-flight validation
Voltage ($U_{K_1,i}$, $U_{K_2,i}$)	±50 nV	Ground based calibration, in-flight validation
Responsivity ($S_{K_1,i}$, $S_{K_2,i}$)	±0.25%	Ground based calibration, in-flight validation
Satellite altitude (z)	±0.1%	Orbital assessment
TSI	±0.5 Wm^{-2}	Space based radiometers observations
d	±0.05%	IMCCE determinations
Qr_i	±0.1%	Calculations, IMCCE determinations
Θ_s	±1%	Deep learning approach

Table 4. ERS technical requirements. For all sensors, it is necessary to monitor the Temperature (T) with a high accuracy to take into account the temperature radiation lost (Stefan–Boltzmann law).

Parameter	Requirements
ERS signal range	$-500\,Wm^{-2}$ to $+1500\,Wm^{-2}$ ($-100\,\mu V$ per Wm^{-2} to $+300\,\mu V$ per Wm^{-2})
ERS resolution	18 bits ($\sim$1.5 nV)
ERS noise detection	$\pm 0.25\,Wm^{-2}$ ($\pm$50 nV)
ERS time response	$<$50 ms
Temperature range	-60 °C to $+90$ °C
Resolution	18 bits ($5.7\,10^{-4}$ °C)
Temperature noise	$< \pm 0.1$ °C
Acquisition time	Better than 10 s

From the ERS sensor error budget (Table 3) and from the knowledge of the TSI absolute uncertainty ($\pm 0.5\,Wm^{-2}$ at 1σ), the expected performances in the absolute determination of OLR and OSR were each $\pm$ 10 Wm^{-2} at 1σ (quadratic summation of uncertainties). Table 5 presents the expected performances from the UVSQ-SAT ERS measurements. The stability per year of the sensors will be demonstrated in orbit and can be compared with other space based measurements.

Table 5. ERS scientific requirements. Total solar irradiance is considered as accurately known.

Parameter	Absolute Uncertainty	Stability per Year
OLR	$\pm 10\,Wm^{-2}$ at 1σ	$\pm 1\,Wm^{-2}$ at 1σ
OSR	$\pm 10\,Wm^{-2}$ at 1σ	$\pm 5\,Wm^{-2}$ at 1σ
TSI	$\pm 0.5\,Wm^{-2}$ at 1σ	$< \pm 0.1\,Wm^{-2}$ at 1σ
EEI = TSI/4 − (OLR + OSR)	$< \pm 15\,Wm^{-2}$ at 1σ	$\sim \pm 5\,Wm^{-2}$ at 1σ

3.2.2. The DEVINS Sensors

To measure with accuracy (see Table 1) the solar spectral irradiance in the Herzberg continuum (200 to 242 nm), we will use disruptive new UVC detectors in Ga_2O_3. Photodetectors based on monoclinic (β) Ga_2O_3 have been demonstrated [3]. With a bandgap of $\sim$4.9 eV β-Ga_2O_3, the films were naturally solar blind without any need for alloying with a third element [41]. Further, it was shown that their spectral response peak could be tuned between about 230 and 255 nm [3] with a bandpass of 40 nm or so at FWHM. These sensors were radiation hard, and do not need cooling, which avoids the associated contaminant trapping/lifetime issues of incumbent devices. Moreover, the gain of these devices is more than two orders of magnitude higher than that of commercial SiC based equivalents. This indicates a potential for operation at lower voltages/powers (only 5 V in the case of UVSQ-SAT). They have a strong responsivity (4A/W), excellent dynamics, and remarkable resistance to radiation. These previous works form a solid basis to implement sensors with adapted characteristics and DEVINS b-Ga_2O_3 based prototypes with a 215–220 nm peak and 40 nm bandpass to cover the Herzberg continuum are currently being developed. These will be small photodiodes using the kind of standardized metal semiconductor package used for transistors and some integrated circuits (base diameter of 8.9 mm, cap diameter of 8.1 mm, cap height of 6.3 mm). They will be designed to measure the UV solar spectral irradiance from a 180 field of view angle with an active area of 1 mm $\times$ 1 mm . They will not require a cooling system to be sensitive to the Herzberg continuum. This aspect should prevent them from degradation due to contamination [33]. They are designed to measure the UV solar spectral irradiance from a 180° field of view angle with an active area of 1 mm $\times$1 mm and a responsivity of $\sim$ 4 A/W. Figure 4 shows the DEVINS photodiodes' manufacturing process. The DEVINS technology will be validated in the framework of the UVSQ-SAT mission (check

in orbit that the detector degradation is weak despite the exposure to radiation (both ionization and displacement-damage effects)). UVSQ-SAT will use a total of four DEVINS photodiodes.

For DEVINS data processing, we will use the six coarse platform photodiodes located on each solar panel for determining the Sun's direction. From the knowledge of the Sun's direction (θ), we will determine the DEVINS solar spectral irradiance (SSI(λ)) from the following instrumental equations based on our experience and history in solar instrumentation developments and observations [42–44].

$$\mathrm{SSI}(\lambda) = \frac{I_d}{S(\lambda, V, T)\ \Sigma\tau(\lambda)\ \cos(\theta)} \left(\frac{f' - d}{f'}\right)^2 \frac{(1\mathrm{u.a.})^2}{d^2} \left(1 - \frac{1}{c}\frac{\partial z}{\partial t}\right)^2 \tag{9}$$

$$\text{and } \frac{1}{f'} = (n-1)\left(\frac{1}{R_1} - \frac{1}{R_2}\right) \tag{10}$$

where I_d is the DEVINS photodiode current measured, $S(\lambda, V, T)$ is the DEVINS photodiode responsivity, which depends on voltage (V) and temperature (T), Σ is the DEVINS photodiode active area, $\tau(\lambda)$ is the DEVINS photodiode transmission of the sapphire window, d is the distance between the DEVINS aperture and the active area, n is the refractive index of the window, and R_1 and R_2 are the curvature radii of the sapphire window lens. A dark current and a flat-field corrections will be necessary for a full correction of the DEVINS data.

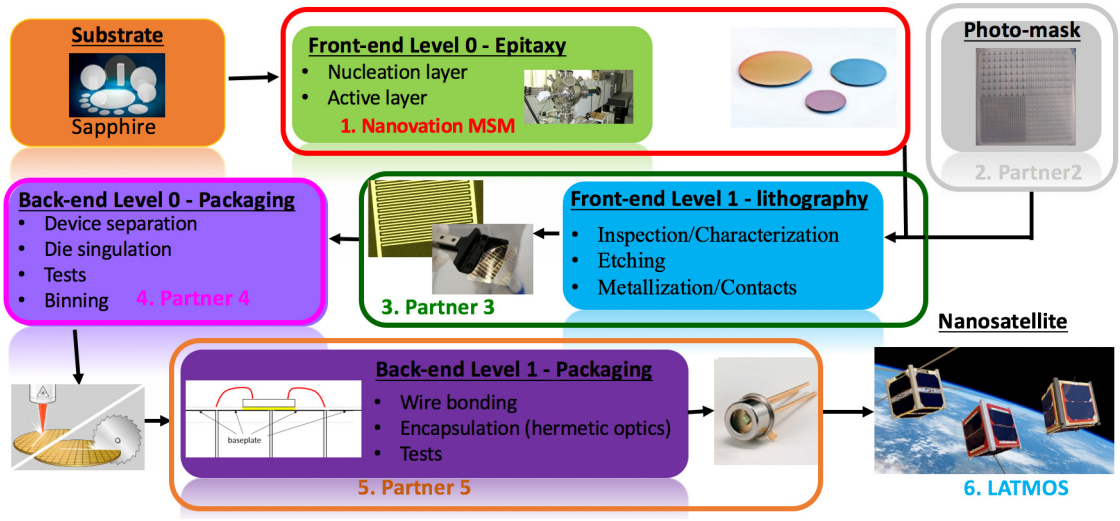

Figure 4. DEVINS manufacturing process. This action, led by LATMOS, is funded by the French Agence Nationale de La Recherche (ANR).

The DEVINS absolute calibration can be performed using the primary standard of spectral irradiance (Physikalisch-Technische Bundesanstalt (Germany) and/or the Laboratory for Atmospheric and Space Physics (LASP) facilities (USA)). The UVSQ-SAT UV SSI expected performances (Table 1) depend mainly on the absolute calibration of the photodiode responsivity ($S(\lambda, V, T)$) and on the DEVINS noise detection. The targeted technical performances of the DEVINS sensors are provided in Table 6, which are compliant with the expected performances in the absolute determination of UV SSI that are of $\pm 2.5\%$ at $1\,\sigma$ in the 200–242 nm spectral region (compatible with uncertainties obtained with SOLAR-ISS spectrum [17]). The stability per year of the DEVINS sensors will be demonstrated in orbit as its low aging in UV.

Table 6. DEVINS photodiodes' technical requirements.

Parameter	Requirements
DEVINS signal range	0 to 2.1 Wm^{-2} (200–242 nm band) Target value: ~1.4 Wm^{-2}
Central wavelength	220 ± 5 nm
Full width at half maximum	20 ± 2 nm
Rejection	10^{-4} in the 250–3000 nm band
DEVINS resolution	18 bits (~0.03 nA)
DEVINS noise detection	< 30 nA
DEVINS time response	< 20 ms
Acquisition integration time	Better than 10 s

3.2.3. The TW Sensor

The Teach' Wear (TW) sensor (50 mm × 25 mm × 8 mm) consists of an inertial measurement unit (a three axis accelerometer and a three axis gyroscope) and a three axis compass (simple type of magnetometer). TW is a new three axis accelerometer/gyroscope/compass, which will be used for determining the attitude of the UVSQ-SAT CubeSat. The main expected TW sensor technical requirements are provided in Table 7.

Table 7. TW sensor technical requirements.

Parameter	Requirements
TW signal range	Accelerometer: ±2 g Gyroscope: ±250 deg Compass: ±4912 µT
TW resolution	16 bits
TW noise detection	Accelerometer: 230 $\mu g/\sqrt{Hz}$ Gyroscope: 0.015 $deg/s/\sqrt{Hz}$
DEVINS time response	<20 ms
Acquisition integration time	10 s

In the framework of the UVSQ-SAT mission, a qualification/validation of the Teach' Wear technology to TRL 9 ("flight proven") will be done through successful mission operations and validation of the expected performances of the TW sensor in space. The TW sensor will be used in the future as medical devices to prevent health problems for astronauts in space. Indeed, astronauts are subjected to serious health problems due to the nature of their jobs, which involve extreme atmospheric conditions and environments, particularly during prolonged space missions.

3.3. The Ground Segment: The UHF/VHF Station

The UVSQ/LATMOS ground station (Figure 5) was implemented using the hardware components recommended by the INSPIRE program [45].

The antenna rig consisted of two circularly polarized Yagi antennas and two rotators, which made it possible to change the elevation and azimuth angles. The antennas were frequency centered on the VHF band (for uplink from ground to space) and UHF band (for downlink from space to ground). The antenna rig is located on the roof of the Observatoire de Versailles Saint-Quentin-en-Yvelines (OVSQ) building, which offers a clear full sky for satellite visibility.

The TS2000 radio was used to transmit RF signals, and a RTL software-defined radio (SDR) was used to receive RF signals. The hardware (i.e., rotators and radio) was controlled through SatPC32 and SDR-Sharp software. Based on the Two Line Elements (TLE), the SatPC32 program allows automatic tracking of the satellite and compensation of the Doppler shift in the radio signal. On the RF transmit line, modulation and AX.25 encapsulation were performed by hardware (i.e., TS2000),

whereas de-modulation and AX.25 de-encapsulation were done by software on the RF receiver line (i.e., RTL-SDR). A custom application was employed to write and read the Consultative Committee for Space Data Systems packet utilization standard (CCSDS PUS) protocol, as well as provide a Graphical User Interface (GUI) to the ground station operator.

Since the UVSQ-SAT CubeSat will use satellite amateur radio frequency bands (i.e., VHF 145.830 MHz and UHF 437.020 MHz), an international frequency coordination is under preparation for being submitted to the International Amateur Radio Union. This will ensure that frequencies are not used by other satellites during the UVSQ-SAT mission, and it will act as an engagement with the amateur radio community. The preparation of the frequency coordination was done with the help of the local Radio-Club (F6KRK) and the AMSAT-Francophone (amateur radio satellite national organization). Thanks to this cooperation, UVSQ-SAT will be able to transmit periodical beacon data, which will be recorded over the world by amateur radio stations.

Figure 5. UVSQ/LATMOS UHF/VHF station (one of the stations of the INSPIRE network). LATMOS hosts students from UVSQ and Paris Saclay universities to provide hands-on experience (satellite manufacturing, antenna realization, etc.).

3.4. UVSQ-SAT Mission Concept of Operations

There are four separate and distinct UVSQ-SAT mission Concepts of the Operation (ConOps) phases:

- Operations before launch and for launch.
- Launch early operations and satellite platform in-orbit verification: deployment of UVSQ-SAT from the CubeSat deployer, automatic activation of the satellite by separation switches, automatic initialization of the onboard software a few seconds after the satellite separation, deployment of deployable structures (antenna), automatic satellite ADCS activation to perform autonomous detumbling of the spacecraft, verification of the link between the ground and satellite, restitution of the satellite orbit thanks to the first visibilities, check that all platform satellite services are running, payload switch-on, and check that all payload instruments are functional.
- Instrument in-orbit verification and operations: preliminary configuration, operational configuration of the satellite, Calibration/Validation (CalVal) of the payload instruments and comparisons with payload ground based calibration (ERS (responsivity, solar absorption (200 to 2500 nm), normal emittance (around 10 μm), bidirectional reflectance distribution function for different angle of incidence, etc.), DEVINS (responsivity, slit function of the sensor, calibrations against national SI standards, etc.), etc.), and validation of the performances. In "routine", the CubeSat will observe the Earth and the Sun full time. Each month, a calibration will be done to characterize the angular responsivity of the sensors (ERS and DEVINS).
- End of life of the UVSQ-SAT CubeSat.

4. Results

This Section presents EEI UVSQ-SAT's expected results and spatial reconstruction of Earth's net radiation. The instrumental requirements for EEI scientific relevance output (absolute uncertainty of $\pm 1\,Wm^{-2}$ at 1σ, stability per decade of $\pm 0.1\,Wm^{-2}$ at 1σ, small spatiotemporal scales with an uncertainty at 1σ of $\pm 1\,Wm^{-2}$ for a 1–10 km resolution) and UVSQ-SAT instrument performances do not match. At the present stage, the UVSQ-SAT CubeSat is a demonstrator, expecting future developments and improvement that would then really allow making use of CubeSat technology for scientific purposes. What are lacking at the present state to obtain accurate relevant EEI absolute value are the extreme cleanliness CubeSat control (careful material selection (e.g., high radiation tolerance, ultra-high vacuum material quality with lowest outgassing values), minimization of organic material (bake-out), and stringent cleanliness procedures of all hardware), intensive CubeSat pre-flight calibration (achieved with detectors and transfer radiation source standards, both traceable to a primary standard source found in synchrotron radiation facilities, while the sensors themselves can be calibrated at the synchrotron facility or locally, at the instrument test facility, by transporting a transfer source standard to that facility), active ADCS, additional narrowband sensors, atomic clock for synchronization, and in-flight calibration to monitor sensors' aging in space. It is important for continuous monitoring of the ERB (as for CERES, EarthCARE, Megha-Tropiques, and Scanner for Radiation Budget (ScaRaB)) and temporal overlap to realize inter-calibrations. It lacks also a high frequency and sampling in measurements and consequently a more accurate determination of the Earth's global energy imbalance along with the diurnal and multi-directional sampling needed to capture spatiotemporal scales. A constellation consisting of small CubeSat's could provide temporal and spatial coverage that are lacking currently to provide accurate EEI measurements and represent important developments that are needed. The UVSQ-SAT mission will contribute to these future developments both in terms of technology advancement (miniaturized sensors used for high scientific relevance) and innovative data processing (reconstruction of a global map of OLR and OSR using multiple sensors' data).

A preliminary analysis of the expected results with a spatial reconstruction of Earth's net radiation that will be obtained with UVSQ-SAT for a given time period of observation was done (Figure 6).

The method used to carry out this study is briefly described below:

1. Use of CERES data ($1^\circ \times 1^\circ$ latitude-longitude geographic grid, monthly mean) to have an initial map of Earth's net radiation for analysis. Then, we considered that this map corresponded to Earth's net radiation "real" map at time t (Figure 6, left upper panel). This map illustrates the fundamental imbalance between net radiation surpluses at the Equator and net radiation deficits at high latitudes.
2. We calculated the UVSQ-SAT CubeSat ground-track (SSO LEO orbit) for a given period (Figure 6, right upper panel).
3. We considered that the maximum angle of view of the UVSQ-SAT sensors can effectively detect the net radiation in a ground area of $1^\circ \times 1^\circ$ along the ground-track and for a given acquisition integration time. Then, we obtained Earth's net radiation associated with the sensors' observations. Finally, we performed an interpolation (Delaunay triangulation) on the scattered dataset that resided in 2D space to obtain Earth's net radiation based on UVSQ-SAT observations for a given time period (Figure 6, left middle and bottom panels).
4. We plotted the differences (Figure 6, right middle and bottom panels) between the "real" map (Figure 6, left upper panel) and the map obtained with the satellite observations for a given period (Figure 6, left middle and bottom panels).

For a one-day observation period, the UVSQ-SAT expected performances were degraded (Figure 6, right middle panel). Earth's net radiation errors with only data processing could be greater than $\pm 30\,Wm^{-2}$ over large geographical areas. Indeed, with an LEO orbit (600 km, 98°), the satellite made just over 14 orbits in a day, and every point on the Earth was covered at least twice. It was clear that it

was insufficient with only one satellite in orbit to cover the entire surface of the Earth (spatial coverage). It took at least 15 days to have a good spatial coverage and to offer a satisfactory Earth net radiation map (Earth's net radiation errors could be greater than $\pm 10\,\mathrm{Wm}^{-2}$ over very small geographical areas), as shown in Figure 6 (right bottom panel).

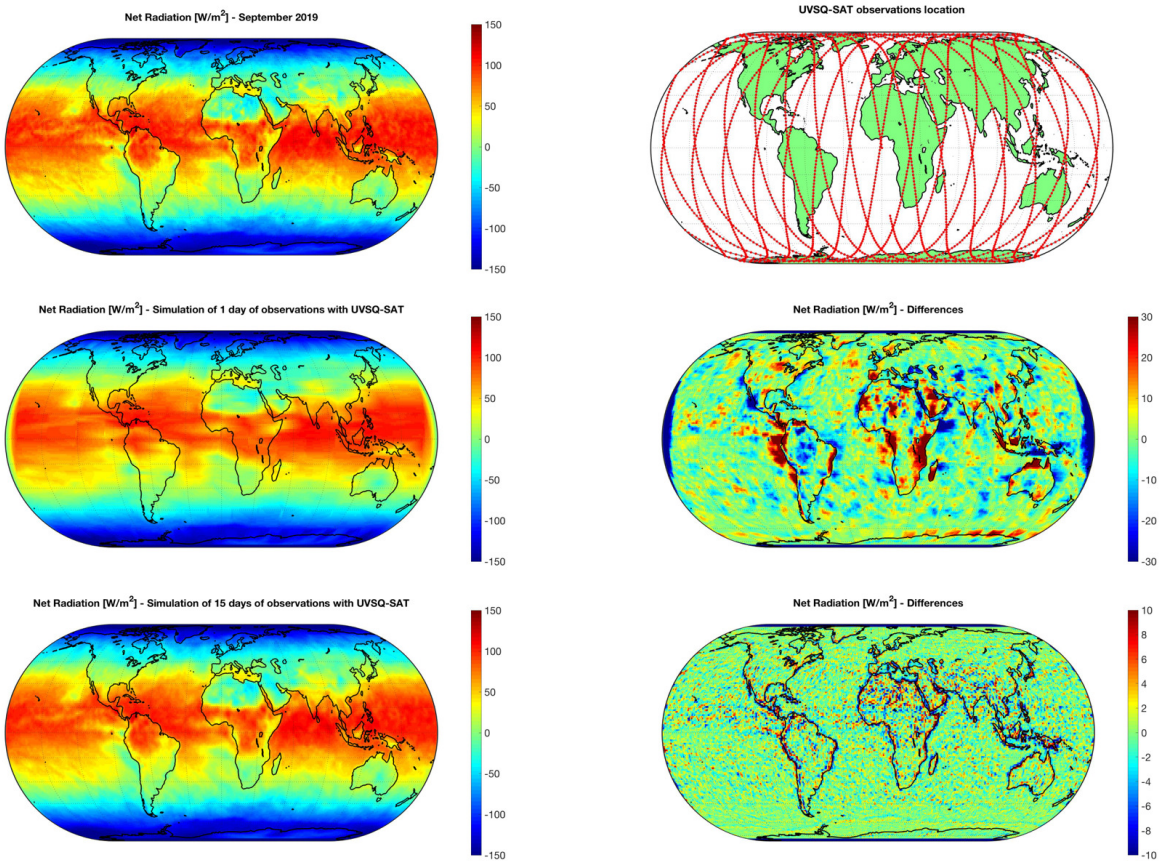

Figure 6. Spatial reconstruction of Earth's net radiation binned into a $1^\circ \times 1^\circ$ latitude-longitude geographic grid that will be obtained with UVSQ-SAT. The source of data for the left upper panel was from CERES observations.

In this case, the result was an average of 15 days. Consequently, we lost the information related to short temporal variations (albedo, clouds, etc.). Indeed, the outgoing shortwave radiation part of the Earth's net radiation is more challenging to measure since it has greater spatial and temporal variability, and it is distributed less evenly around the Earth. For example, sharp edges in albedo (e.g., clouds) are intricate and evolve quickly [8].

5. Final Discussion

The analysis done in Section 4 highlighted the interest to implement a satellite constellation to measure the true Earth's energy imbalance, since only satellite observations of net radiation flux variability at TOA can provide information at shorter timescales.

Figure 7 shows the daily Earth net radiation as a function of longitude for different terrestrial latitudes (real observations (o) and simulated (s) using a constellation of 15 satellites during a day of observations). With a constellation of 15 satellites (inclinations of 30°, 45°, 60°, 75°, and 98.5° and LTAN of 02:30, 10:30, and 18:30), one could have excellent EEI measurements during a day of observation. A constellation of 50 satellites would allow accurate measurements of the Earth's energy imbalance (errors less than $\pm 1\,\mathrm{Wm}^{-2}$) with the diurnal and multi-directional sampling, which are a prerequisite to capture spatio-temporal variations (e.g., every three hours and ideally a few km resolution).

Long term measurements are required using satellite constellations with recovery periods (inter-calibrations) for multi-decadal observations to track Earth's energy imbalance over time for predicting the future course of global warming and verifying that the measures taken for the climate are effective. Accurate annual net radiation figures from pole to pole are required and represent key scientific indicators. There is a net energy surplus at the Equator and a net energy deficit at the poles (see Figure 6, top left panel), so energy will flow from the Equator to poles. This energy is transferred poleward as latent and sensible heat (warm ocean water and warm, moist air move poleward, while cooler water and cooler, drier air move toward the Equator). The Equator-versus-pole energy imbalance is the fundamental driver of atmospheric and oceanic circulation. From UVSQ-SAT and its future constellation (Figure 8), we propose to monitor this parameter. In the case of a satellite constellation, the instrumental calibration (pre-flight calibration with the same primary standard source, in-flight calibration to monitor aging with the same process) aspects will have to be studied in detail to guarantee accuracy and precision for each satellite. Indeed, the determination of top of atmosphere global net radiation budget using broadband non-scanner instruments remains complex due to outstanding calibration challenges [46].

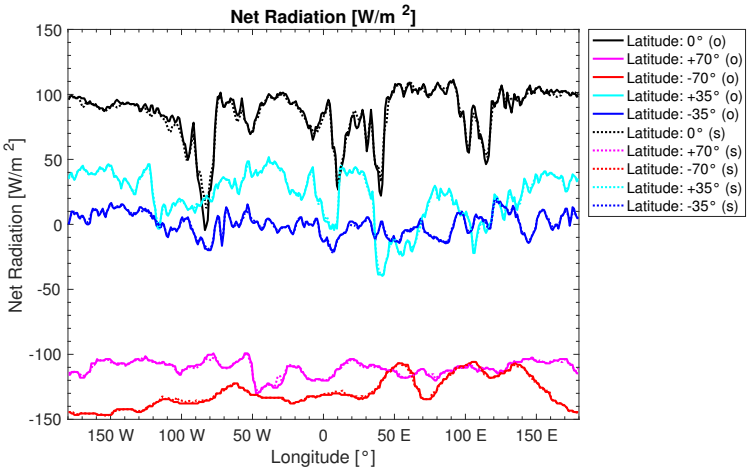

Figure 7. Daily Earth net radiation as a function of longitude for different terrestrial latitudes. (o) represents the real observations (CERES data). (s) represents the results obtained with a simulation of observations from a virtual constellation of 15 satellites (five different inclinations and three different LTAN).

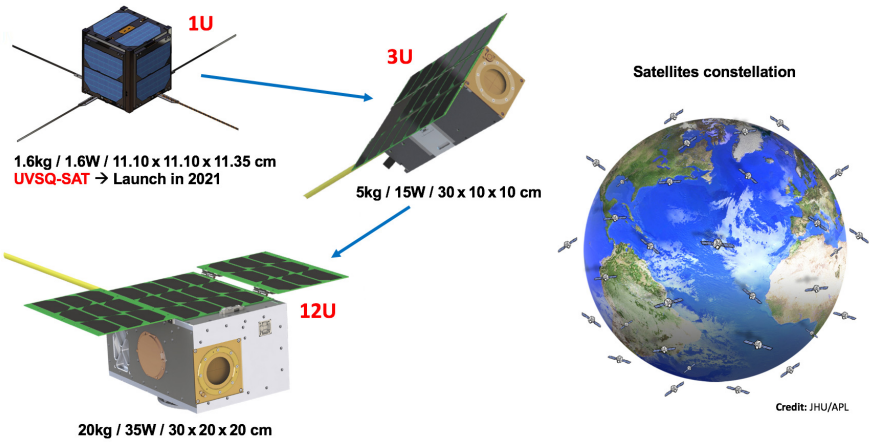

Figure 8. From a very simple unitary CubeSat to an increasingly complex nanosatellite on which a small satellite constellation will be based.

6. Conclusions

UVSQ-SAT is a scientific and technology demonstration satellite in the domain of Earth observation and solar physics, scheduled to be launched in 2020/2021. The main scientific goals are to measure the top of atmosphere outgoing longwave radiation and shortwave radiation and the solar spectral irradiance in the Herzberg continuum (200–242 nm) with good accuracy. UVSQ-SAT uses disruptive technologies for remote sensing and will improve the miniaturization and compactness of small sensors onboard small satellites. The UVSQ-SAT tools are used in our education program to train students in space technology, Earth observations, and astronomy and astrophysics. UVSQ-SAT represents a CubeSat of the INSPIRE series of satellite missions. The INSPIRE program is a multinational consortium of universities collaborating to develop a constellation of small satellites for cutting edge space and Earth science research, a supporting global ground station network, as well as research and educational programs covering spacecraft design, space systems engineering, operations, and data analysis.

Currently, the UVSQ-SAT mission is not intended to provide a continuity of the essential climate variables' data records. However, the use of small compact space qualified sensors like those used in UVSQ-SAT can facilitate future innovative space programs onboard small satellites and the implementation of a future small satellite constellation dedicated to the measurements of the essential climate variables with full data traceability. The advantages of such a future constellation have been described in this manuscript and allow considering exceptional revisit time and spatial resolution, in particular for the Earth's energy imbalance monitoring. Indeed, a constellation of 50 satellites is needed to estimate global daily mean top of atmosphere outgoing longwave radiation and shortwave radiation. Moreover, this satellite constellation is the best way to observe diurnal cycles. These observations are more easily realized by flying the Earth radiation budget instruments on less expensive CubeSats than with classic satellites. Several UVSQ-SAT CubeSats represent a possible tool to meet the EEI global daily mean and the diurnal cycle.

Author Contributions: Conceptualization, M.M. (Mustapha Meftah), L.D., P.K., S.B., A.S., A.H., E.B., S.A., C.D., P.G., L.L., A.J.-V., X.A., N.M., J.P.-C., T.L., G.P., D.R., P.B., É.S., F.T., A.P., K.S., A.B.A., M.M. (Michel Mahé), C.M., A.A., L.C., A.C., P.-R.D., and A.B.; science (climate studies and solar physics), M.M. (Mustapha Meftah), L.D., P.K., S.B., A.S., A.H., and P.-R.D.; hardware and engineering, M.M. (Mustapha Meftah), É.B., S.A., C.D., P.G., L.L., A.J.-V., X.A., N.M., J.P.-C., T.L., G.P., D.R., P.B., É.S., F.T., A.P., K.S., A.B.A., M.M. (Michel Mahé), C.M., A.A., L.C., A.C.; methodology, M.M. (Mustapha Meftah); software, M.M (Mustapha Meftah)., A.H., C.D., and A.J.-V.; formal analysis, M.M. (Mustapha Meftah), L.D., P.K., S.B., A.S., and A.H; resources, M.M. (Mustapha Meftah), L.D., P.K., S.B., A.S., A.H., E.B., S.A., C.D., P.G., L.L., A.J.-V., X.A., N.M., J.P.-C., T.L., G.P., D.R., P.B., É.S., F.T., A.P., K.S., A.B.A., M.M. (Michel Mahé), C.M., A.A., L.C., A.C., P.-R.D., and A.B.; writing, original draft preparation, M.M. (Mustapha Meftah), L.D., P.K., S.B., A.S., and A.H; writing, review and editing, M.M. (Mustapha Meftah), P.K., and S.B.; project administration, M.M. (Mustapha Meftah), L.D., P.K., S.B., A.S., A.H, and E.B.; funding acquisition, M.M. (Mustapha Meftah), P.K., A.S., L.D., and J.P.-C. All authors have read and agreed to the published version of the manuscript.

Funding: This research was mainly funded by UVSQ (Université de Versailles Saint-Quentin-en-Yvelines, France), Agence Nationale de La Recherche (ANR, France), and Centre National de la Recherche Scientifique (CNRS, France).

Acknowledgments: The UVSQ-SAT team acknowledges support from the Université de Versailles Saint-Quentin-en-Yvelines (UVSQ, France), the Sorbonne Université (SU, France), the Université Paris-Saclay (France), the Centre National de la Recherche Scientifique (CNRS, France), the Centre National d'Études Spatiales (CNES, France), the Laboratory for Atmospheric and Space Physics (LASP, USA), the National Central University (NCU, Taiwan), the Nanyang Technological University (NTU, Singapore), and French Small and Middle Enterprises (Carta-Rouxel, Nanovation, ACRI-ST). The UVSQ-SAT team gratefully acknowledges David Orlikowski (Director of the Centre d'investigation clinique et d'innovation technologique (CIC 1429, France)) and Frederic Barbot (Coordinator of the CIC 1429) for their support in the development of the TW sensor. The authors thankfully acknowledge l'Observatoire de Paris (France) and Exploration Spatiale des Environnements Planétaires (ESEP, France) for their support.

Conflicts of Interest: The authors declare no conflict of interest.

Appendix A

UVSQ-SAT consists of several subsystems such as the mechanical structure, the power subsystem, the thermal control subsystem, the attitude determination and control system (ADCS), the command and data handling subsystem (CDHS), the communication subsystem and the payload subsystem (ERS, DEVINS, and the 3-axis accelerometer/gyroscope/compass (TW sensor)).

The UVSQ-SAT CubeSat structure is compliant with the CubeSat standard and is compatible with the ISIPOD or Quadpack CubeSat deployer. Two separation switches are part of the satellite structure. These ensure that the UVSQ-SAT CubeSat is inactive during launch and pre-launch activities. All UVSQ-SAT materials and coating selection, must be compliant with specific requirements such as total mass loss (TML) less than 1% and collected volatile condensable material (CVCM) less than 0.1%, according to guidelines for spacecraft cleanliness control (ESA-PSS-51 from European Space Agency).

The Electric Power Supply (iEPS) is designed to support the power conversion, storage and distribution to the UVSQ-SAT CubeSat subsystems. The iEPS provides 3 max power point tracking (MPPT) for power conversion up to 25 W. This system would improve the amount of power supplied to the batteries of the CubeSat. The MPPTs make sure the attached solar panel cells are operated at a voltage that yields maximum power, which increases efficiency with respect to other EPS that use fixed point voltage for the solar panels. iEPS includes 2-batteries pack (22.5 Wh), which regulates the voltage to several outputs (3.3 V, 5 V, and unregulated battery line (6–8 V)) through multiple switchable and permanent power lines. Fully charged battery corresponds to 0% depth of discharge (DOD). Ideally, 30% DOD or less is recommended full time. UVSQ-SAT has 6 ISIS solar panels made up of 12 Azurspace solar cells at high efficiency (30% for beginning of life (BOL)), which allow a solar power conversion of up to 2.2 W per 1 U area in low Earth orbit.

The UVSQ-SAT ADCS contains a set of 6 photodiodes located on the solar panels (coarse estimation of the Sun's direction) and a magnetorquer board (iMTQ) with 3 magnetic actuators in 3-axis for providing actuation of 0.2 Am^2 (for limit the tumbling, which typically will occur as soon as the CubeSat will be deployed). UVSQ-SAT does not have a system that allows a satellite pointing in a specific direction.

The CDHS subsystem with the onboard computer (OBC) will process, distribute, command, store and format data (master of the I^2C bus with the different platform subsystems and the payload, high storage capacity embedded with the two SD-cards, joint test action group (JTAG) interface for debugging, etc.). It consists of a motherboard (iOBC) and a daughterboard (DB). The iOBC electronic motherboard interfaces with the UVSQ-SAT daughter board (DB), which is a custom design for the UVSQ-SAT project. The daughterboard is used on the UVSQ-SAT platform for interfacing with the external sensors of the platform (6 temperature sensors and 6 coarse photodiodes) and for interfacing with the payload electronic board (8 general purpose input/output (GPIO) pins, serial peripheral interface (SPI) data line). There is also an interface system that allows among other things to connect the electronic boards between them using the 104-pin CubeSat kit bus (CSKB) connectors.

Because of satellite tumbling and low power range, radio-communications are a challenge. UVSQ-SAT uses a VHF/UHF transceiver (TRXVU), which is a full-duplex VHF/UHF radio system. It offers an uplink capability of 9.6 kbps (FSK modulation) and a downlink rate of up to 9.6 kbps (BPSK modulation). The electronic board uses radio link layer protocol AX.25. The deployable antenna system contains two tape spring antennas of up to ∼60 cm in length in the case of VHF and two tape spring antennas up to ∼20 cm in length in the case of UHF. This antenna system is located at the bottom side of the UVSQ-SAT satellite along the Z direction (Figure 2). This subsystem uses a power supply for deployment in orbit and will be automatic. Each antenna element can be deployed separately through a dual redundant deployment system. The antenna is designed to cover the amateur satellite band with a UHF selection of 437.020 MHz and VHF of 145.830 MHz being validated by International Amateur Radio Union (IARU).

References

1. Meftah, M.; Keckhut, P.; Damé, L.; Bekki, S.; Sarkissian, A.; Hauchecorne, A. Think the way to measure the Earth Radiation Budget and the Total Solar Irradiance with a small satellites constellation. In Proceedings of the Sensors and Systems for Space Applications XI, Orlando, FL, USA, 16–17 April 2018; Volume 10641, p. 106410S. [CrossRef]
2. Trenberth, K.E.; Fasullo, J.T. Tracking Earth's Energy. *Science* **2010**, *328*, 316–317. [CrossRef] [PubMed]
3. Rogers, D.J.; Bove, P.; Arrateig, X.; Sandana, V.E.; Teherani, F.H.; Razeghi, M.; McClintock, R.; Frisch, E.; Harel, S. The new oxide paradigm for solid state ultraviolet photodetectors. In Proceedings of the Oxide-Based Materials and Devices IX, San Francisco, CA, USA, 28 January–1 February 2018; Volume 10533, p. 105331P. [CrossRef]
4. Blunden, J.; Arndt, D.S. State of the Climate in 2018. *Bull. Am. Meteorol. Soc.* **2019**, *100*, Si-S306. [CrossRef]
5. Hansen, J.; Nazarenko, L.; Ruedy, R.; Sato, M.; Willis, J.; Del Genio, A.; Koch, D.; Lacis, A.; Lo, K.; Menon, S.; et al. Earth's Energy Imbalance: Confirmation and Implications. *Science* **2005**, *308*, 1431–1435. [CrossRef] [PubMed]
6. von Schuckmann, K.; Palmer, M.D.; Trenberth, K.E.; Cazenave, A.; Chambers, D.; Champollion, N.; Hansen, J.; Josey, S.A.; Loeb, N.; Mathieu, P.P.; et al. An imperative to monitor Earth's energy imbalance. *Nat. Clim. Chang.* **2016**, *6*, 138–144. [CrossRef]
7. Meyssignac, B.; Boyer, T.; Zhao, Z.; Hakuba, M.Z.; Landerer, F.W.; Stammer, D.; Köhl, A.; Kato, S.; L'Ecuyer, T.; Ablain, M.; et al. Measuring Global Ocean Heat Content to Estimate the Earth Energy Imbalance. *Front. Mar. Sci.* **2019**, *6*, 432. [CrossRef]
8. Swartz, W.; Lorentz, S.; Papadakis, S.; Huang, P.; Smith, A.; Deglau, D.; Yu, Y.; Reilly, S.; Reilly, N.; Anderson, D. RAVAN: CubeSat Demonstration for Multi-Point Earth Radiation Budget Measurements. *Remote Sens.* **2019**, *11*, 796. [CrossRef]
9. Hansen, J.; Sato, M.; Kharecha, P.; von Schuckmann, K. Earth's energy imbalance and implications. *Atmos. Chem. Phys.* **2011**, *11*, 13421–13449. [CrossRef]
10. Stephens, G.L.; Li, J.; Wild, M.; Clayson, C.A.; Loeb, N.; Kato, S.; L'Ecuyer, T.; Stackhouse, P.W.; Lebsock, M.; Andrews, T. An update on Earth's energy balance in light of the latest global observations. *Nat. Geosci.* **2012**, *5*, 691–696. [CrossRef]
11. Allan, R.P.; Liu, C.; Loeb, N.G.; Palmer, M.D.; Roberts, M.; Smith, D.; Vidale, P.L. Changes in global net radiative imbalance 1985–2012. *Geophys. Res. Lett.* **2014**, *41*, 5588–5597. [CrossRef]
12. Wild, M.; Ohmura, A.; Schär, C.; Müller, G.; Folini, D.; Schwarz, M.; Hakuba, M.Z.; Sanchez-Lorenzo, A. The Global Energy Balance Archive (GEBA) version 2017: A database for worldwide measured surface energy fluxes. *Earth Syst. Sci. Data* **2017**, *9*, 601–613. [CrossRef]
13. Johnson, G.C.; Lyman, J.M.; Loeb, N.G. Improving estimates of Earth's energy imbalance. *Nat. Clim. Chang.* **2016**, *6*, 639–640. [CrossRef]
14. Loeb, N.G.; Doelling, D.R.; Wang, H.; Su, W.; Nguyen, C.; Corbett, J.G.; Liang, L.; Mitrescu, C.; Rose, F.G.; Kato, S. Clouds and the Earth's Radiant Energy System (CERES) Energy Balanced and Filled (EBAF) Top-of-Atmosphere (TOA) Edition-4.0 Data Product. *J. Clim.* **2018**, *31*, 895–918. [CrossRef]
15. IPCC. Summary for Policymakers. In *Climate Change 2013: The Physical Science Basis. Contribution of Working Group I to the Fifth Assessment Report of the Intergovernmental Panel on Climate Change*; Stocker, T., Qin, D., Plattner, G.K., Tignor, M., Allen, S., Boschung, J., Nauels, A., Xia, Y., Bex, V., Midgley, P., Eds.; Book Section SPM; Cambridge University Press: Cambridge, UK; New York, NY, USA, 2013; pp. 1–30. [CrossRef]
16. Zelinka, M.D.; Randall, D.A.; Webb, M.J.; Klein, S.A. Clearing clouds of uncertainty. *Nat. Clim. Chang.* **2017**, *7*, 674–678. [CrossRef]
17. Meftah, M.; Damé, L.; Bolsée, D.; Hauchecorne, A.; Pereira, N.; Sluse, D.; Cessateur, G.; Irbah, A.; Bureau, J.; Weber, M.; et al. SOLAR-ISS: A new reference spectrum based on SOLAR/SOLSPEC observations. *Astron. Astrophys.* **2018**, *611*, A1. [CrossRef]
18. Gray, L.J.; Beer, J.; Geller, M.; Haigh, J.D.; Lockwood, M.; Matthes, K.; Cubasch, U.; Fleitmann, D.; Harrison, G.; Hood, L.; et al. Solar Influences on Climate. *Rev. Geophys.* **2010**, *48*, RG4001. [CrossRef]
19. Adolphi, F.; Muscheler, R.; Svensson, A.; Aldahan, A.; Possnert, G.; Beer, J.; Sjolte, J.; Björck, S.; Matthes, K.; Thiéblemont, R. Persistent link between solar activity and Greenland climate during the Last Glacial Maximum. *Nat. Geosci.* **2014**, *7*, 662–666. [CrossRef]

20. Field, C.; Barros, V.; Mach, K.; Mastrandrea, M.; Aalst, M.; Adger, W.; Arent, D.; Barnett, J.; Betts, R.; Bilir, T.; et al. Technical Summary. In *Climate Change 2014: Impacts, Adaptation, and Vulnerability. Part A: Global and Sectoral Aspects*; Cambridge University Press: Cambridge, UK, 2015; Volume 1, pp. 35–94.
21. Flato, G.; Marotzke, J.; Abiodun, B.; Braconnot, P.; Chou, S.C.; Collins, W.; Cox, P.; Driouech, F.; Emori, S.; Eyring, V.; et al. Evaluation of climate models. In *Climate Change 2013: The Physical Science Basis. Contribution of Working Group I to the Fifth Assessment Report of the Intergovernmental Panel on Climate Change*; Stocker, T.F., Qin, D., Plattner, G.K., Tignor, M., Allen, S.K., Doschung, J., Nauels, A., Xia, Y., Bex, V., Midgley, P.M., Eds.; Cambridge University Press: Cambridge, UK, 2013; pp. 741–882. [CrossRef]
22. Roth, R.; Joos, F. A reconstruction of radiocarbon production and total solar irradiance from the Holocene ^{14}C and CO_2 records: Implications of data and model uncertainties. *Clim. Past* **2013**, *9*, 1879–1909. [CrossRef]
23. Steinhilber, F.; Beer, J. Prediction of solar activity for the next 500 years. *J. Geophys. Res. (Space Phys.)* **2013**, *118*, 1861–1867. [CrossRef]
24. Ermolli, I.; Matthes, K.; Dudok de Wit, T.; Krivova, N.A.; Tourpali, K.; Weber, M.; Unruh, Y.C.; Gray, L.; Langematz, U.; Pilewskie, P.; et al. Recent variability of the solar spectral irradiance and its impact on climate modelling. *AtmChemPhys* **2013**, *13*, 3945. [CrossRef]
25. Sukhodolov, T.; Rozanov, E.; Ball, W.T.; Bais, A.; Tourpali, K.; Shapiro, A.E.I.; Telford, P.; Smyshlyaev, S.; Fomin, B.; Sander, R.; et al. Evaluation of simulated photolysis rates and their response to solar irradiance variability. *J. Geophys. Res. (Atmospheres)* **2016**, *121*, 6066–6084. [CrossRef]
26. Thiéblemont, R.; Marchand, M.; Bekki, S.; Bossay, S.; Lefèvre, F.; Meftah, M.; Hauchecorne, A. Sensitivity of the tropical stratospheric ozone response to the solar rotational cycle in observations and chemistry-climate model simulations. *Atmos. Chem. Phys.* **2017**, *17*, 9897–9916. [CrossRef]
27. Arsenovic, P.; Rozanov, E.; Anet, J.; Stenke, A.; Schmutz, W.; Peter, T. Implications of potential future grand solar minimum for ozone layer and climate. *Atmos. Chem. Phys.* **2018**, *18*, 3469–3483. [CrossRef]
28. Kodera, K.; Kuroda, Y. A possible mechanism of solar modulation of the spatial structure of the North Atlantic Oscillation. *J. Geophys. Res. (Atmospheres)* **2005**, *110*, D02111. [CrossRef]
29. Matthes, K.; Kuroda, Y.; Kodera, K.; Langematz, U. Transfer of the solar signal from the stratosphere to the troposphere: Northern winter. *J. Geophys. Res. (Atmospheres)* **2006**, *111*, D06108. [CrossRef]
30. Chiodo, G.; Calvo, N.; Marsh, D.R.; Garcia-Herrera, R. The 11 year solar cycle signal in transient simulations from the Whole Atmosphere Community Climate Model. *J. Geophys. Res. (Atmospheres)* **2012**, *117*, D06109. [CrossRef]
31. Swartz, W.H.; Stolarski, R.S.; Oman, L.D.; Fleming, E.L.; Jackman, C.H. Middle atmosphere response to different descriptions of the 11-yr solar cycle in spectral irradiance in a chemistry-climate model. *Atmos. Chem. Phys. Discuss.* **2012**, *12*, 7039–7071. [CrossRef]
32. Richard, E.; Harber, D.; Drake, G.; Rutkowsi, J.; Castleman, Z.; Smith, M.; Sprunck, J.; Zheng, W.; Smith, P.; Fisher, M.; et al. Compact spectral irradiance monitor flight demonstration mission. In Proceedings of the SPIE, San Diego, CA, USA, 11–15 August 2019; Volume 11131, p. 1113105. [CrossRef]
33. Meftah, M.; Dominique, M.; BenMoussa, A.; Dammasch, I.E.; Bolsée, D.; Pereira, N.; Damé, L.; Bekki, S.; Hauchecorne, A. On-orbit degradation of recent space-based solar instruments and understanding of the degradation processes. In Proceedings of the SPIE, Anaheim, CA, USA, 9–13 April 2017; Volume 10196, p. 1019606. [CrossRef]
34. BenMoussa, A.; Gissot, S.; Schühle, U.; Del Zanna, G.; Auchère, F.; Mekaoui, S.; Jones, A.R.; Walton, D.; Eyles, C.J.; Thuillier, G.; et al. On-Orbit Degradation of Solar Instruments. *Sol. Phys.* **2013**, *288*, 389–434. [CrossRef]
35. Brasseur, G.P.; Solomon, S. *Aeronomy of the Middle Atmosphere: Chemistry and Physics of the Stratosphere and Mesosphere*; Springer: New York, NY, USA, 2005; p. 3.
36. Meftah, M.; Bolsée, D.; Damé, L.; Hauchecorne, A.; Pereira, N.; Bekki, S.; Cessateur, G.; Foujols, T.; Thiéblemont, R. Solar Irradiance from 165 to 400 nm in 2008 and UV Variations in Three Spectral Bands During Solar Cycle 24. *Sol. Phys.* **2016**, *291*, 3527–3547. [CrossRef]
37. Yeo, K.L.; Krivova, N.A.; Solanki, S.K.; Glassmeier, K.H. Reconstruction of total and spectral solar irradiance from 1974 to 2013 based on KPVT, SoHO/MDI, and SDO/HMI observations. *Astron. Astrophys.* **2014**, *570*, A85. [CrossRef]
38. Solanki, S.K.; Krivova, N.A.; Haigh, J.D. Solar Irradiance Variability and Climate. *Annu. Rev. Astron. Astrophys.* **2013**, *51*, 311–351. [CrossRef]

39. Puig-Suari, J.; Schoos, J.; Turner, C.; Wagner, T.; Connolly, R.; Block, R.P. CubeSat developments at Cal Poly: The standard deployer and PolySat. In Proceedings of the SPIE 4136, Small Payloads in Space, San Diego, CA, USA, 7 November 2000; Volume 4136, pp. 72–78. [CrossRef]
40. Twiggs, R.J. Space system developments at Stanford University: From launch experience of microsatellites to the proposed future use of picosatellites. In Proceedings of the SPIE 4136, Small Payloads in Space, San Diego, CA, USA, 7 November 2000; Volume 4136, pp. 79–86. [CrossRef]
41. Razeghi, M.; Park, J.H.; McClintock, R.; Pavlidis, D.; Teherani, F.H.; Rogers, D.J.; Magill, B.A.; Khodaparast, G.A.; Xu, Y.; Wu, J.; et al. A review of the growth, doping, and applications of Beta-Ga_2O_3 thin films. In Proceedings of the SPIE International Society for Optics and Photonics, Oxide-based Materials and Devices IX, San Francisco, CA, USA, 27 January–1 February 2018; Volume 10533, pp. 21–44. [CrossRef]
42. Meftah, M.; Dewitte, S.; Irbah, A.; Chevalier, A.; Conscience, C.; Crommelynck, D.; Janssen, E.; Mekaoui, S. SOVAP/Picard, a Spaceborne Radiometer to Measure the Total Solar Irradiance. *Sol. Phys.* **2014**, *289*, 1885–1899. [CrossRef]
43. Bolsée, D.; Pereira, N.; Gillotay, D.; Pandey, P.; Cessateur, G.; Foujols, T.; Bekki, S.; Hauchecorne, A.; Meftah, M.; Damé, L.; et al. SOLAR/SOLSPEC mission on ISS: In-flight performance for SSI measurements in the UV. *Astron. Astrophys.* **2017**, *600*, A21. [CrossRef]
44. Meftah, M.; Bamas, É.; Cambournac, P.; Cherabier, P.; Demarets, R.; Denis, G.; Dion, A.; Duroselle, R.; Duveiller, F.; Eichner, L.; et al. SERB, a nano-satellite dedicated to the Earth-Sun relationship. In Proceedings of the SPIE 9838, Sensors and Systems for Space Applications IX, Baltimore, MD, USA, 17–21 April 2016; Volume 9838, p. 98380T. [CrossRef]
45. Chandran, A.; Baker, D. INSPIRING a new generation of University small satellite missions for space science. In Proceedings of the EGU General Assembly Conference Abstracts, Vienna, Austria, 7–12 April 2019; p. 12179.
46. Wong, T.; Smith, G.L.; Kato, S.; Loeb, N.G.; Kopp, G.; Shrestha, A.K. On the Lessons Learned From the Operations of the ERBE Nonscanner Instrument in Space and the Production of the Nonscanner TOA Radiation Budget Data Set. *IEEE Trans. Geosci. Remote Sens.* **2018**, *56*, 5936–5947. [CrossRef]